Environ Sci Pollut Res
DOI 10.1007/s11356-016-7681-2

Sol-gel synthesis of TiO_2 nanoparticles: effect of Pluronic P123 on particle's morphology and photocatalytic degradation of paraquat

Cédric B. D. Marien[1,2] · **Clément Marchal**[1] · **Alain Koch**[3] · **Didier Robert**[1] · **Patrick Drogui**[2]

Received: 21 June 2016 / Accepted: 12 September 2016

Abstract We report a facile method to tune TiO_2 nanoparticles' morphology by modifying and an acid-catalyzed sol-gel synthesis with Pluronic P123. Synthesized particles were characterized by transmission electron microscopy, BET analysis, and X-ray diffraction spectroscopy. XRD analysis revealed a high anatase content while BET measurements showed that porous volume strongly depends on the amount of P123. We demonstrate that high amounts of P123 increase particle's aspect-ratio from spherical to rod-shape morphology. We evaluated the photocatalytic performances for the removal of methyl viologen (paraquat) and found that best performances are obtained for the following weight ratio $P123/TiO_2 = 7.5$. Furthermore, P25 is less active than synthesized nanoparticles.

Keywords Photocatalysis · Sol-gel · TiO_2 nanoparticles · Nanorods · Methyl viologen

Responsible editor: Philippe Garrigues

Electronic supplementary material The online version of this article (doi:10.1007/s11356-016-7681-2) contains supplementary material, which is available to authorized users.

✉ Cédric B. D. Marien
cdric.ma@gmail.com

[1] Institut de Chimie et Procédés pour l'Energie, l'Environnement et la Santé (ICPEES), CNRS-UMR7515-University of Strasbourg, Saint-Avold Antenna, Université de Lorraine, 12 rue Victor Demange, 57500 Saint-Avold, France

[2] Institut national de la recherche scientifique (INRS-Terre et Environnement), Université du Québec, 490 rue de la Couronne, Québec City G1K 9A9, Canada

[3] IUT Moselle-Est, département Chimie de Saint-Avold, Université de Lorraine, rue Victor Demange, 57500 Saint-Avold, France

Introduction

Water pollution by organic contaminants is a worldwide problem due to the increasing number of emerging contaminants with a negative impact on the environment. Many organics are released by various industries in many fields: agricultural (pesticides, herbicides, fertilizers), dye industry, pharmaceuticals, cosmetic/personal care products, plasticizers, and various industrial additives.

Current water treatment plants with classical primary (flocculation/decantation) and secondary (biological treatment) steps are not sufficiently efficient to remove completely every organic contaminants. Indeed, some compounds are not separated/degraded by these two steps (Carra et al. 2014). Hence, new processes are required as tertiary step to improve the overall efficacy of water treatment plants.

Advanced oxidation processes (AOPs) are very suitable as tertiary treatment due to their ability to produce highly oxidizing species, especially the hydroxyl radical (OH·) (Andreozzi 1999). Among these processes, photocatalysis has been studied for more than 40 years to remove organic pollutants (Hashimoto et al. 2007). This process is based on the absorption of light by a semiconductor, usually TiO_2, to produce electron-hole pairs, reacting at the interface to produce oxidizing species such as hydroxyl or superoxide radical. Hydroxyl radicals have been deemed to be the major active species during the photocatalytic oxidation reaction. The production of these radicals can be detected by photoluminescence spectroscopy using a probe molecule (coumarin or terephtalic acid) producing stable oxidized products (Ishibashi et al. 2000; Gomes et al. 2005). Coumarin is usually employed because it is non-fluorescent and its oxidized by-product (7-hydroxycoumarin) is fluorescent (Louit et al. 2005; Newton and Milligan 2006; Xiang et al. 2011). Hence, the production of OH· radicals is correlated to the concentration of

Published online: 23 September 2016

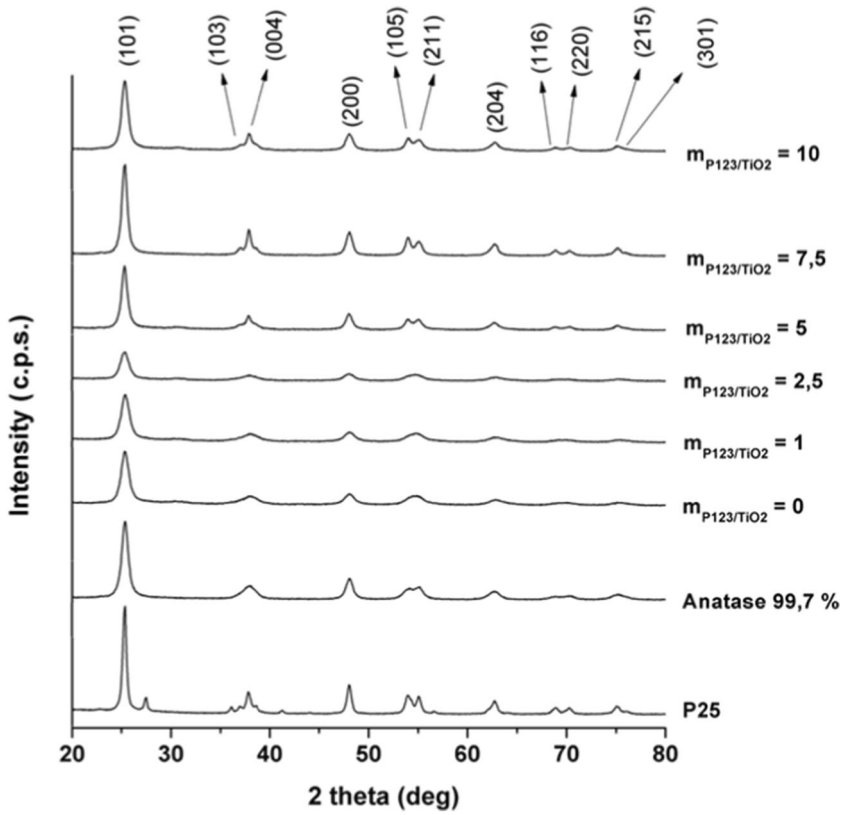

Fig. 1 XRD pattern for the various samples

fluorescent by-products. Other methods like electron-spin resonance (ESR) allow to detect paramagnetic species like the OH radical (Wang et al. 2011; He et al. 2014). However, the lifetime of OH radical is so short that scavengers like DMPO (Nosaka et al. 2003) or TEMPO (He et al. 2014) must be employed. Stable adducts are then detected (DMPO-OH or TEMPO-OH) by ESR to find the amount of OH radicals produced. This ability to produce OH radicals make photocatalysis very suitable for the non-selective removal of organic pollutants in waste water.

TiO_2 has been intensively studied for its high photocatalytic activity, high stability against photocorrosion, and its low cost. Moreover, a very interesting feature of photocatalysis is its ability to decompose organic pollutant in water as well as in gas phase. In order to improve the photocatalytic activity of TiO_2, many researchers developed nanomaterials with different shapes to tune their catalytic activity: nanoparticles (Peng et al. 2005), nanowires (Jitputti et al. 2008), nanofibers (Christoforidis et al. 2015), nanotubes (Marien et al. 2016). Among existing synthesis, the sol-gel method is very suitable to produce nanomaterials because it does not require complex installations and the synthesis proceeds under ambient pressure and temperature. Sol-gel synthesis is based on the hydrolysis/condensation of a titanium precursor to produce a sol and then a gel. Subsequently, after solvent evaporation, a xerogel is obtained which is milled and heat treated to produce highly crystalline TiO_2 nanopowders.

Titanium precursors are usually very reactive species with water, especially titanium tetraisopropoxide. In order to obtain a better control during the hydrolysis/condensation steps, complexing agents are usually employed to improve precursor's stability toward water (Livage et al. 1988). Acetic acid has been recognized to improve titanium precursor's stability (Livage et al., 1989). Indeed, acetate ions act as chelating agents with titanium precursor and increase its coordination number and hence its stability.

It is well recognized that increasing the accessible surface area of a TiO_2 photocatalyst can promote the adsorption and diffusion of reactants so that improved photocatalytic performances are obtained (Wen et al. 2015). In order to increase the active surface area, pore formers are usually added to the sol-

Table 1 XRD angles and corresponding FWHM and crystallite size

Sample	2 theta (deg)	FWHM (deg)	Crystallite size (nm)
P25	25.31	0.437	21
mP123/TiO_2 = 0	25.39	0.937	9.8
mP123/TiO_2 = 1	25.37	0.979	9.4
mP123/TiO_2 = 2.5	25.30	1.035	8.9
mP123/TiO_2 = 5	25.31	0.723	12.7
mP123/TiO_2 = 7.5	25.31	0.648	14.2
mP123/TiO_2 = 10	25.31	0.767	12

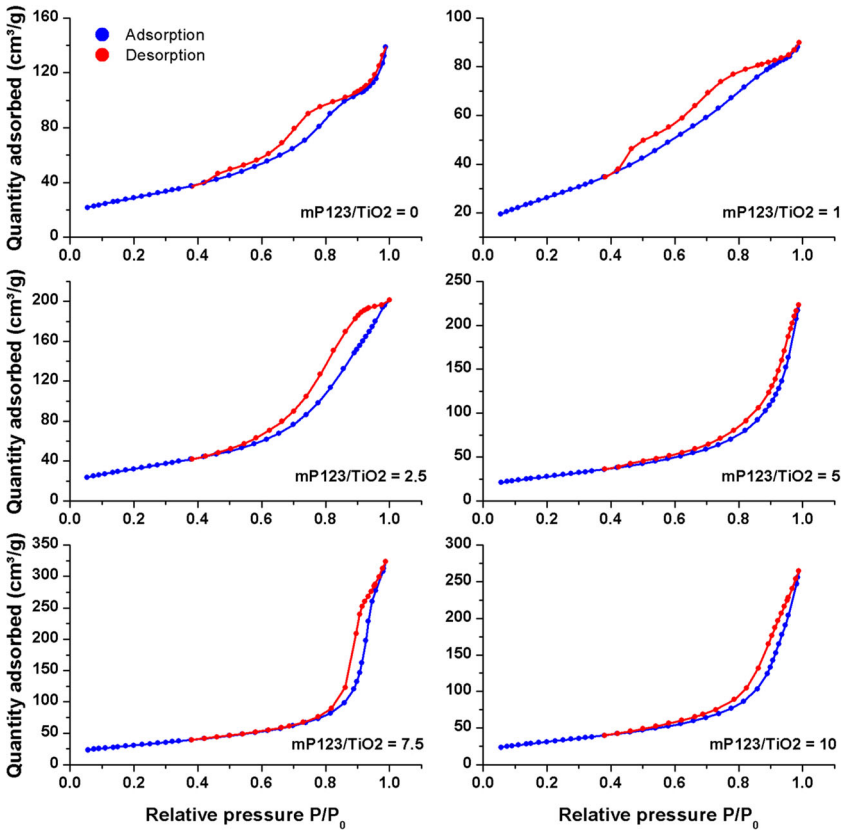

Fig. 2 BET isotherms

gel synthesis. Hard- and soft-template synthesis have been widely reported in the literature to produce a porous structures. Indeed, hard templates are attractive because a high degree of self-organization can be obtained, for example, with inverse-opals by using templating nanoparticles (e.g., silica or polystyrene particles) (Lee et al. 2004; Zhao et al. 2006). However, the hard template technique requires the synthesis of nanoparticles which is not cost effective. On the other hand, the soft template synthesis using polymers is relatively simple and does not require complex synthesis used in the hard template procedure. In the soft template synthesis, a polymeric precursor is added to the sol and the porosity is created by removal of the polymeric chains by high temperature annealing to produce mesoporous anatase or rutile particles. For this purpose, many polymeric precursors have been employed in the literature to increase the photocatalytic activity of TiO_2 nanoparticles: PEG (Bu et al. 2004; Bu et al., 2005; Jahromi et al. 2009), P123 (Tian et al. 2002; Calleja et al. 2004; Myilsamy et al. 2015; Yang et al. 2016). Here, we modified an acid catalyzed sol-gel synthesis with various ratios of a soft template (Pluronic P123) to increase the active surface area and improve the photocatalytic performances. The photocatalytic activity of the synthesized nanoparticles was studied for the removal of paraquat dichloride. This compound, also known as 1,1′-Dimethyl-4,4′-bipyridinium, is a widely used herbicide commercialized as "Gramoxone." This compound has been forbidden in the European Union due to its high toxicity and its low lethal doses: 35 mg/kg (Organization 1984; Dinis-Oliveira et al. 2008). However, it is still used in more than 100 countries. This pollutant is very simple to follow by UV-vis spectroscopy at 257 nm (Moctezuma et al. 1999). Hence, experimental photocatalytic degradation were followed at this wavelength to compare the synthesized nanoparticles with commercially available P25 (Evonik).

Experimental part

Synthesis of the photocatalyst

The synthesis were performed as follows: first, solution A was prepared by mixing 3 ml titanium tetra-isopropoxide (97 % Aldrich) and 10.6 ml of anhydrous ethanol (99.8 % Aldrich)

Table 2 Textural properties of the as-synthesized nanoparticles

mP123/TiO_2	Active surface area (m^2/g)	Porous volume (cm^3/g)	Pore diameter (nm)
0	106	0.21	7.6
1	96	0.13	5.5
2.5	121	0.32	8.6
5	100	0.34	13.5
7.5	113	0.50	17.39
10	115	0.41	13.8

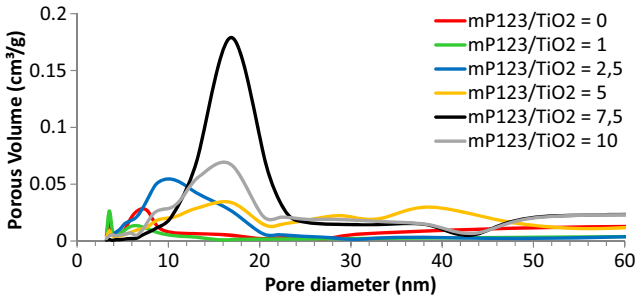

Fig. 3 Evolution of pore diameter and porous volume with the amount of Pluronic P123 in the as-synthesized nanoparticles

while solution B contained 0.3 ml anhydrous ethanol, 0.15 ml distilled water, and 11.1 ml of acetic acid (99.7 % Aldrich). Solution B was then added drop by drop into solution A to obtain a clear transparent sol. After a few hours, the sol becomes milky and after several hours a gel is obtained. Subsequently, a drying step at 110 °C is performed during 24 h to remove volatile solvents and then a xerogel is obtained and milled in an agate mortar. The resulting powder is calcined at 450 °C during 2 h (5 °C/min). To improve this synthesis, we studied the influence of various ratios of Pluronic P123 (Aldrich). The following weight ratios were studied: mass P123/TiO_2 = 0, 1; 2.5; 5; 7.5; and 10.

Characterization

Transmission electron microscopy was performed on a JEOL 2100F at 200 kV. A Shimadzu Miniflex II was used for X-ray diffraction measurements and a Micromeritics ASAP 2420 for BET analysis operating at 77 K. Thermogravimetric analysis were performed with Setaram Labsys Evo.

Photocatalytic tests were performed in a solar simulator Ametek CPS+ with a Xenon Lamp. Typically 100 mg of TiO_2 powder were immersed in a cooled recipient at 20 °C with 100 ml of paraquat (10 ppm). First, the suspension was left in the dark during 1 h to reach adsorption equilibrium. Then, light was turned on and 2 ml of suspensions were taken at various time intervals. TiO_2 was removed from solution with a 0.45 μm filter and paraquat's concentration was measured by UV-vis spectrophotometer (Biochrom Libra S12).

Results and discussion

XRD analysis

XRD diffractograms of TiO_2 samples with various P123 ratios are presented in Fig. 1. A very high anatase content is observed for the as-synthesized nanoparticles compared to the reference sample (99.7 % of anatase, Aldrich). Indeed, no rutile peaks were found. This is due to the heat treatment at 450 °C which is known to produce a high anatase content (source). We chose this calcination temperature because anatase has a better photocatalytic activity due to the higher electron-hole pair lifetime compared to rutile (Zhang et al. 2014). Zhang et al. attribute this difference of activity, between anatase and rutile, to the direct/indirect bandgap behavior of these phases (Zhang et al. 2014). Indeed, it was shown that anatase behaves as an indirect semiconductor; thus,

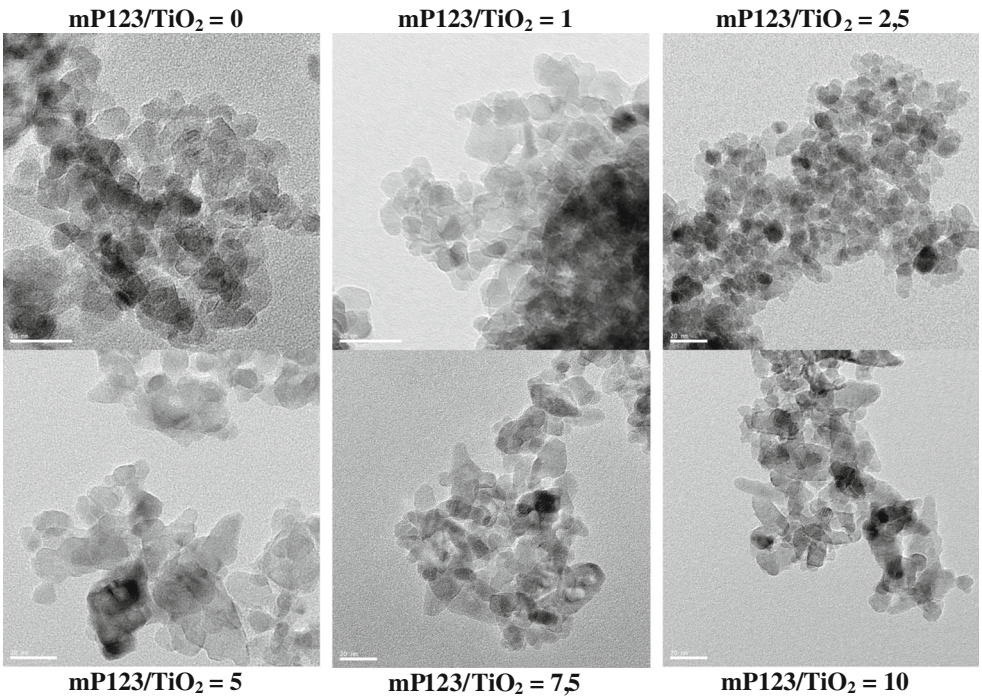

Fig. 4 Transmission electron microscopy of as-synthesized nanoparticles

electron desexcitation from the conduction band to the valence band is forbidden by selection rules. Hence, electron-hole lifetime is higher with anatase while rutile acts as a direct semiconductor with a lower carrier lifetime.

We can see that the main peak (101) appears at 25.3°. Its intensity and FWHM strongly depends on the synthesis conditions. Assuming the Debye-Scherer equation to be valid (spherical particles), we obtain the crystallite size for each sample with the following equation:

$$S_{hKl} = \frac{K\lambda}{b\ \cos\theta}$$

With s_{hkl} the average crystallite size for the hkl peak in Angström, K the Scherer constant (0.89), λ the incident X-ray wavelength (1.5406 Angström), θ the Bragg diffraction angle, and b the FWHM. The average crystallite size is presented in Table 1. We can see that crystallite sizes are very close for low P123 content (ratio 0; 1; and 2.5) whereas a slight increase is obtained for higher P123 content with a maximum around 7.5.

BET analysis

Nitrogen adsorption/desorption isotherms are given in Fig. 2. Isotherms present a type IV behavior characteristic of

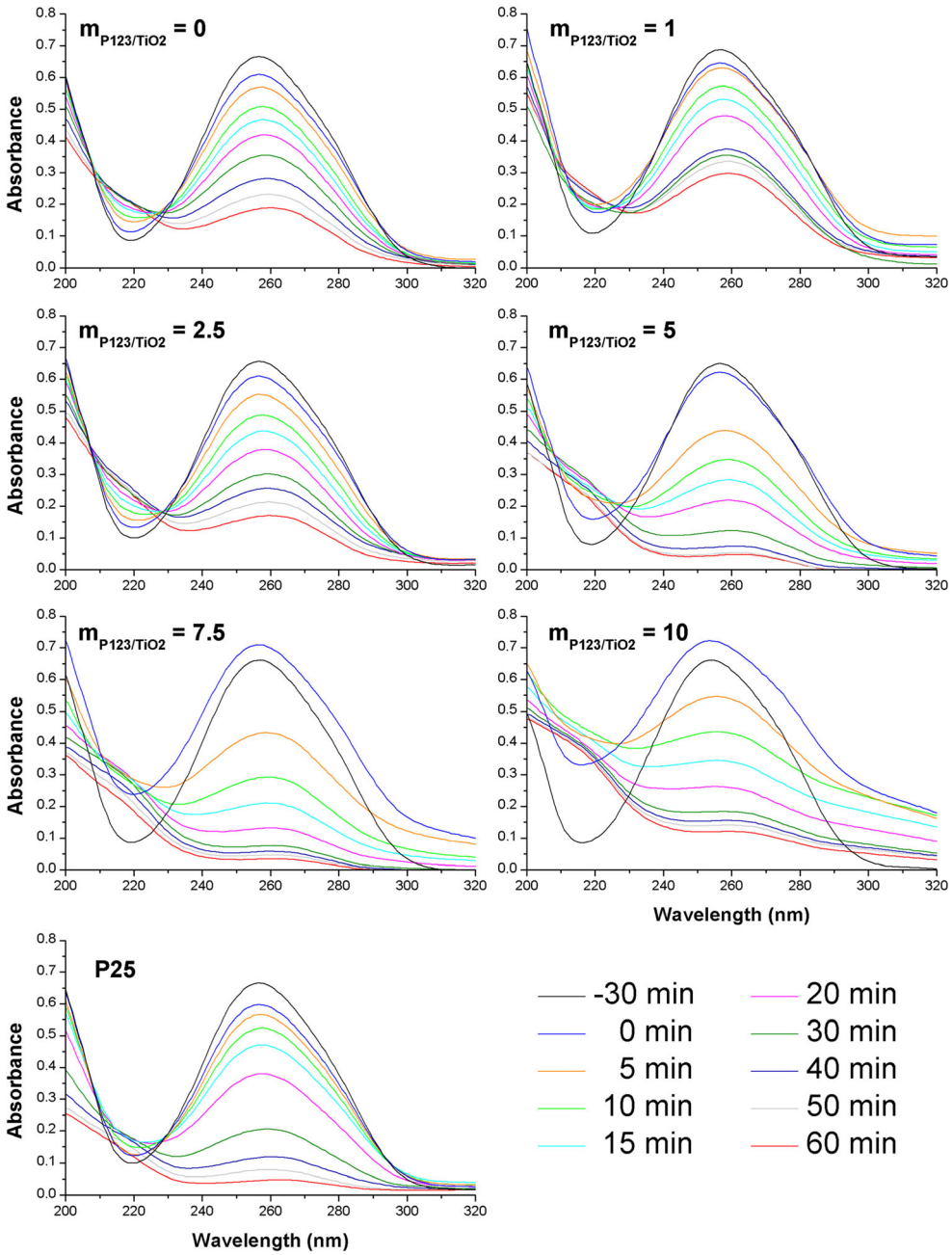

Fig. 5 Photocatalytic degradation of paraquat followed by UV-vis spectroscopy

mesoporous materials. We can see that the porous volume strongly depends on the P123 loading.

Active surface area, porous volume, and average pore size are presented in Table 2:

BET surface area is poorly affected by P123 loading. However, we can see that porous volume is maximal for the 7.5 ratio with approximately 3000 cm^3/g which is twice higher than without P123 (Fig. 3). Consequently, P123 loading do not influence strongly the BET area but induce a higher porous volume. BJH analysis on the desorption curves give the correlation between the porous volume and the pore diameter.

Without P123, two pore sizes are detected at 4 and 7.5 nm. When P123 is added, the pore size distribution is shifted to larger pore diameters ($5 < \times < 25$ nm). In conclusion, while BET surface shows few differences, BJH porosity strongly depends on the P123 content with a maximum value for $mP123/TiO_2 = 7.5$. In order to have a better understanding of the influence of P123 loading on particle's morphology, TEM analysis were performed.

TEM analysis

Figure 4 presents the transmission electron microscope images of the synthesized samples. It can be seen that particles synthesized with low P123 content (<5) are nearly round-shaped while higher amounts of P123 induce deformations, particles become rod-shaped. Hence, deviations from the Debye-Scherer equation can be expected for crystallite size calculation. Moreover, it is quite complicated to obtain a particle size distribution due to the evolving morphology with increasing P123 amount.

Photocatalytic tests

Photocatalytic tests show that paraquat is degraded by every sample (Fig. 5). However, the kinetic strongly depends on the amount of P123. The absorbance at 257 nm is mainly attributed to paraquat. However, some by-products such as monopyridone and dipyridone can absorb around this wavelength as shown by Moctezuma et al. (Moctezuma et al. 1999).

Samples with a high P123 content present a global increase of absorbance in the 200–250 nm region after 30 min in the dark. We believe that this increase correspond to residues of Pluronic P123 not consumed during heat treatment at 450 °C. Thermogravimetric analysis confirms this observation (see supplementary information). Indeed approximately 3 % of Pluronic P123 residues are still present in the sample at 450 °C under ambient air. These residues should explain the slight increase of absorbance at $t = 0$ min for $mP123/TiO_2 = 5$; 7.5; and 10 where the quantity of P123 is significant compared to lower ratios ($mP123/TiO_2 = 0$, 1, and 2.5).

Figure 6 presents the photocatalytic degradation for each sample after several time intervals. We can see that high ratios of P123 in the sol-gel tend to increase the photocatalytic activity.

Since the BET surface area is approximately the same for those particles, we believe that particle's morphology can be an explanation to rationalize the different photocatalytic activities. Indeed, it is well known that exposed facets at the surface of a catalyst strongly influences the catalytic activity. Since the morphology evolves from spherical to rod-shape, we can attribute the change in photocatalytic activity to the modification of particle's morphology with P123.

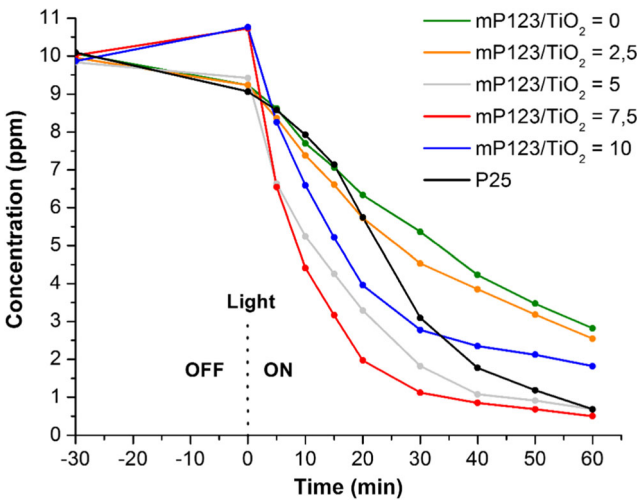

Fig. 6 Degradation of paraquat through time

Conclusion

We successfully synthesized TiO_2 nanoparticles with a high anatase content and showed that Pluronic P123 acts as a pore former which tends to increase the porous volume. Contrary to all expectations, BET surface area is poorly affected by Pluronic P123. However, it was shown that particle's morphology is highly dependent on the P123 content in the sol-gel, and transitions from spherical to rod-shape were observed. Furthermore, photocatalytic performances were dependent on particle's morphology and higher photocatalytic activities were obtained compared to commercial P25 nanoparticles.

References

Andreozzi R (1999) Advanced oxidation processes (AOP) for water purification and recovery. Catal Today 53:51–59. doi:10.1016/S0920-5861(99)00102-9

Bu S, Jin Z, Liu X et al (2004) Fabrication of TiO2 porous thin films using peg templates and chemistry of the process. Mater Chem Phys 88: 273–279. doi:10.1016/j.matchemphys.2004.03.033

Bu SJ, Jin ZG, Liu XX et al (2005) Synthesis of TiO2 porous thin films by polyethylene glycol templating and chemistry of the process. J Eur Ceram Soc 25:673–679. doi:10.1016/j.jeurceramsoc.2003.12.025

Calleja G, Serrano D, Sanz R (2004) Study on the synthesis of high-surface-area mesoporous TiO2 in the presence of nonionic surfactants. Ind Eng Chem Res 2485–2492. doi:10.1021/ie030646a

Carra I, Sanchez Perez JA, Malato S et al (2014) Performance of different advanced oxidation processes for tertiary wastewater treatment to remove the pesticide acetamiprid. J Chem Technol Biotechnol 91: 72–81. doi:10.1002/jctb.4577

Christoforidis KC, Sengele A, Keller V, Keller N (2015) Single-step synthesis of SnS < inf > 2</inf > Nanosheet-decorated TiO < inf > 2</inf > Anatase nanofibers as efficient photocatalysts for the degradation of gas-phase diethylsulfide. ACS Appl Mater Interfaces 7:19324–19334. doi:10.1021/acsami.5b05370

Dinis-Oliveira RJ, Duarte JA, Sánchez-Navarro A et al (2008) Paraquat poisonings: mechanisms of lung toxicity, clinical features, and treatment. Crit Rev Toxicol 38:13–71. doi:10.1080/10408440701669959

Gomes A, Fernandes E, Lima JLFC (2005) Fluorescence probes used for detection of reactive oxygen species. J Biochem Biophys Methods 65:45–80. doi:10.1016/j.jbbm.2005.10.003

Hashimoto K, Irie H, Fujishima A (2007) A historical overview and future prospects. AAPPS Bull 17:12–28. doi:10.1007/BF00290457

He W, Liu Y, Wamer WG, Yin J-J (2014) Electron spin resonance spectroscopy for the study of nanomaterial-mediated generation of reactive oxygen species. J Food Drug Anal 22:49–63. doi:10.1016/j.jfda.2014.01.004

Ishibashi KI, Fujishima A, Watanabe T, Hashimoto K (2000) Detection of active oxidative species in TiO2 photocatalysis using the fluorescence technique. Electrochem Commun 2: 207–210. doi:10.1016/S1388-2481(00)00006-0

Jahromi HS, Taghdisian H, Afshar S, Tasharrofi S (2009) Effects of pH and polyethylene glycol on surface morphology of TiO2 thin film. Surf Coatings Technol 203:1991–1996. doi:10.1016/j.surfcoat.2009.01.034

Jitputti J, Suzuki Y, Yoshikawa S (2008) Synthesis of TiO2 nanowires and their photocatalytic activity for hydrogen evolution. Catal Commun 9:1265–1271. doi:10.1016/j.catcom.2007.11.016

Lee J, Han S, Hyeon T (2004) Synthesis of new nanoporous carbon materials using nanostructured silica materials as templates. 478–486

Livage J, Henry M, Sanchez C (1988) Sol-gel chemistry of transition metal oxides. Prog Solid State Chem 18:259–341. doi:10.1016/0079-6786(88)90005-2

Livage J, Sanchez C, Henry MDS (1989) The chemistry of the sol gel process. Solid State Ionics 33:633–638

Louit G, Foley S, Cabillic J et al (2005) The reaction of coumarin with the OH radical revisited: hydroxylation product analysis determined by fluorescence and chromatography. Radiat Phys Chem 72:119–124. doi:10.1016/j.radphyschem.2004.09.007

Marien CBD, Cottineau T, Robert D, Drogui P (2016) TiO2 nanotube arrays: influence of tube length on the photocatalytic degradation of paraquat. Appl Catal B Environ 194:1–6. doi:10.1016/j.apcatb.2016.04.040

Moctezuma E, Leyva E, Monreal E et al (1999) Photocatalytic degradation of the herbicide "Paraquat.". Chemosphere 39:511–517

Myilsamy M, Mahalakshmi M, Murugesan V, Subha N (2015) Enhanced photocatalytic activity of nitrogen and indium co-doped mesoporous TiO < inf > 2</inf > nanocomposites for the degradation of 2,4-dinitrophenol under visible light. Appl Surf Sci 342:1–10. doi:10.1016/j.apsusc.2015.03.017

Newton GL, Milligan JR (2006) Fluorescence detection of hydroxyl radicals. Radiat Phys Chem 75:473–478. doi:10.1016/j.radphyschem.2005.10.011

Nosaka Y, Komori S, Yawata K et al (2003) Photocatalytic •OH radical formation in TiO2 aqueous suspension studied by several detection methods. Phys Chem Chem Phys 5:4731–4735. doi:10.1039/b307433a

Organization WH (1984) Paraquat and diquat. International Programme on Chemical Safety

Peng T, Zhao D, Dai K et al (2005) Synthesis of titanium dioxide nanoparticles with mesoporous anatase wall and high photocatalytic activity. J Phys Chem B 109:4947–4952. doi:10.1021/jp044771r

Tian B, Yang H, Liu X et al (2002) Fast preparation of highly ordered nonsiliceous mesoporous materials via mixed inorganic precursors. Chem Commun (Camb):1824–1825. doi:10.1039/b205006d

Wang Z, Ma W, Chen C et al (2011) Probing paramagnetic species in titania-based heterogeneous photocatalysis by electron spin resonance (ESR) spectroscopy—a mini review. Chem Eng J 170:353–362. doi:10.1016/j.cej.2010.12.002

Wen J, Li X, Liu W et al (2015) Photocatalysis fundamentals and surface modification of TiO2 nanomaterials. Cuihua Xuebao/Chinese J Catal 36:2049–2070. doi:10.1016/S1872-2067(15)60999-8

Xiang Q, Yu J, Wong PK (2011) Quantitative characterization of hydroxyl radicals produced by various photocatalysts. J Colloid Interface Sci 357:163–167. doi:10.1016/j.jcis.2011.01.093

Yang G, Ding H, Chen D et al (2016) A simple route to synthesize mesoporous titania from TiOSO4: influence of the synthesis conditions on the structural, pigments and photocatalytic properties. Appl Surf Sci 376:227–235. doi:10.1016/j.apsusc.2016.03.156

Zhang J, Zhou P, Liu J, Yu J (2014) New understanding of the difference of photocatalytic activity among anatase, rutile and brookite TiO2. Phys Chem Chem Phys 16:20382–20386. doi:10.1039/C4CP02201G

Zhao XS, Su F, Yan Q et al (2006) Templating methods for preparation of porous structures. J Mater Chem 16:637. doi:10.1039/b513060c